

An Embarrassingly Simple Defense Against Backdoor Attacks On SSL

Aryan Satpathy^{*1}

aryandityan5@gmail.com

Nilaksh^{*1}

nilaksh404@kgpian.iitkgp.ac.in

Dhruba Rajwade^{*1}

rajwadedhruva@kgpian.iitkgp.ac.in

¹Indian Institute of Technology, Kharagpur

Abstract

Self Supervised Learning (SSL) has emerged as a powerful paradigm to tackle data landscapes with absence of human supervision. The ability to learn meaningful tasks without the use of labeled data makes SSL a popular method to manage large chunks of data in the absence of labels. However, recent work indicates SSL to be vulnerable to backdoor attacks, wherein models can be controlled, possibly maliciously, to suit an adversary's motives. [11] introduce a novel frequency-based backdoor attack: CTRL. They show that CTRL can be used to efficiently and stealthily gain control over a victim's model trained using SSL. In this work, we devise two defense strategies against frequency-based attacks in SSL: One applicable before model training and the second to be applied during model inference. Our first contribution utilizes the invariance property of the downstream task to defend against backdoor attacks in a generalizable fashion. We observe the ASR (Attack Success Rate) to reduce by over 60% across experiments. Our Inference-time defense relies on evasiveness of the attack and uses the luminance channel to defend against attacks. Using object classification as the downstream task for SSL, we demonstrate successful defense strategies that do not require re-training of the model. Code is available at <https://github.com/Aryan-Satpathy/Backdoor>.

1. Introduction

Self supervised learning (SSL) has become ubiquitous in many machine learning tasks, largely owing to the work of [1], [7], and [2]. The ability of SSL to learn good quality representations without any human supervision makes it a powerful paradigm that has also been shown to attain performance on par with supervised methods ([5]). Contrastive learning is a popular flavor of SSL, where similarity is generated using the input training data itself (poten-

tially through augmentations as shown by [1], [7], [2] and [26]), and a model is constrained to learn such an embedding space in which similar samples stay close to each other while dissimilar ones are far apart.

Recently, [11] demonstrated a simple yet potent poison insertion strategy (CTRL) for SSL, by perturbing images in the *frequency* space to poison a small fraction of the data (1% of the entire training dataset). This poisoning method, being implemented in the frequency domain of the image, is invisible to the human eye and hard to detect via existing defense mechanisms. Additionally, this method is *augmentation invariant*, making it highly effective against SSL. In this work, we explore the problem of defending against frequency-based backdoor attacks, in which a malicious entity plants “backdoors” into target models during training and activates such backdoors at inference. We demonstrate our defense strategy against frequency-based attacks using CTRL, but also theoretically show that our defense is partly generalizable on other types of attacks.

2. Related work:

Backdoor attacks and defenses have been extensively studied in Deep Learning, especially in supervised settings. The goal of attacks is to cause “controlled misclassification” of a model in a way that suits the attacker.

Backdoor Attacks: Backdoor attacks can be described as poisoning a small subset of training data with trigger-embedded target class inputs, where a trigger is a manual perturbation introduced by the attacker to create a mapping between the trigger and the target class. A lot of work has been done in designing triggers to increase backdoor efficiency. [6] introduce a pixel-based trigger for model backdooring. [3] use a blended injection strategy to generate triggers, where a trigger pattern is partially added to the target image, with a magnitude such that its effect is quite potent as a backdoor, but it remains visibly obscure. Inspired from stenography, [12] demonstrate a trigger strategy using Least Significant Bit (LSB) substitution to

^{*}These authors contributed equally to this work

create sub-pixel perturbations which are indistinguishable to the human eye, but can be detected using neural networks (allowing for the trigger pattern to get associated with the target class). [14] introduce a trigger strategy tailored for contrastive learning, by concatenating multiple input images to create poisoned inputs, and repeating this process iteratively to end up with a poisoned dataset such that two augmentations of poisoned images produce features similar to target class images. [17] show how simple augmentations considered standard for SSL can be converted into triggers. [4] (FIBA) and [11] (CTRL) demonstrate highly effective backdoor attacks using frequency-domain triggers.

Backdoor Defenses: A variety of backdoor defense strategies exist that aim towards detecting poisoned samples, recovering clean samples from poisoned samples, or reverse-engineering the poison to mitigate its effect on the trained encoder or the downstream task. [24] identified the first generalizable strategy to detect as well as '*un-poison*' poisoned samples. They detect poisoned samples by considering the minimum perturbation required to transform an output label to the target, and reverse-engineer the trigger pattern to obtain clean samples. [10] identify poisoned samples by differential clustering on trained backdoored models. [21] regenerate the poison pattern by a two-step process where first, they build a robust classifier through a de-noising diffusion process, then iteratively synthesize the poison pattern by iteratively optimizing the cross-entropy between the target class and robust classifier outputs. [16] use controlled layer-wise weight initialization and knowledge distillation to defend using unlabelled data. [13], [25] also utilize knowledge-distillation to defend against backdoored models.

Backdoors and SSL: SSL methods have recently been shown to be vulnerable to backdoor attacks through model access ([9]) or via poisoning a small subset of the training data ([19]). [11] (CTRL) demonstrate a highly successful attack against SSL. [19] also demonstrates a primitive defense against backdoor attacks, while [22] displays a more comprehensive method to detect poisoned samples in SSL.

3. Preliminaries

3.1. Self-supervised and contrastive learning

In SSL, an encoder f is trained on input data D using supervisory signals generated using D itself, which allows for high-quality representations to be learned from data without any labels. Roughly speaking, contrastive learning aims to map two views (or augmentations) of the same input to two similar feature vectors. Using it is preferred while working in unsupervised settings or SSL.

3.2. Equivariance and invariance

Inspired from [15], we use *Equivariance* and *Invariance* to defend against backdoor attacks at training time. Let \mathbf{x} be an input image. A neural network produces a representation $\mathbf{h} = F_\theta(\mathbf{x})$ for the input image. A function(F_θ)'s equivariance and invariance properties are determined as follows:

$$\begin{aligned} \text{Equivariance: } & F_\theta(\mathbf{x}) = g^{-1} \circ F_\theta \circ g(\mathbf{x}) \\ \text{Invariance: } & F_\theta(\mathbf{x}) = F_\theta \circ g(\mathbf{x}) \end{aligned} \quad (1)$$

where \circ represents composition, g is a transformation and $g^{-1}(\cdot)$ denotes its inverse.

Whether to use Equivariance or Invariance property depends on the downstream task. Generally, for Segmentation and Object Detection tasks, one may use the *equivariance* condition (i.e, for example, while rotating the input image, label masks also have to be rotated in the exact same way), but for our downstream task (Classification), we use the *invariance* condition (i.e, for example, even after rotating the input image, the classification label remains the same). Exceptions to the mentioned rule include tasks like MNIST classification, where rotating an image containing the digit '6' might end up becoming the digit '9'.

We demonstrate the (augmentation) invariant nature of our downstream task by implementing and including results for [4] and [18] attacks. The triggers used in these attacks lack (augmentation) invariance and therefore plummet when used against SSL.

3.3. Luma channel

Human vision exhibits a finer spatial sensitivity to the luminance of an image but changes in chrominance are not nearly as easily perceptible. This inherent property allows for the implementation of chroma subsampling, a widely utilized technique in image and video systems to store chromatic information at lower resolutions, thereby reducing the necessary bandwidth ([23]). However, this perceptual characteristic can also be exploited for steganography, involving the covert concealment of data within images ([20], [8]).

$$Y' = 0.2126R' + 0.7152G' + 0.0722B' \quad (2)$$

In video and digital photography, the luminance channel or luma is often denoted by Y' , and is common in color spaces like $Y'CbCr$, $Y'PbPr$ and $Y'UV$. Luma represents the achromatic part of the image, while the other channels contain the color information. Luma is a weighted sum (Eq. 2) of the gamma-corrected *RGB* components of an image, $R'G'B'$.

4. Methods

Attacker threat model: Following the threat model from [19] and [11], we assume that the attacker can pollute a

small fraction of the training dataset. The attacker has no information about the training regime or network architecture used by the victim.

Defender assumptions: We assume that the defender has full control over training procedure. The defender doesn't require access to a small subset of clean dataset, which is often required for existing defenses based on knowledge distillation eg: [13], [25].

4.1. Gaussian blur: an embarrassingly simple yet potent defense

A poisoned image (\tilde{x}) usually contains a constant trigger pattern t . Due to its constant nature, the trigger pattern t provides the model with a *path of least variance*; that is, as compared to learning all the variations of the target class present in the dataset, the model finds it easier to associate t to the target class. In order to diminish the efficacy of poison at training time, one must increase the variance of t in the poisoned images. The model will no longer have a pattern that is easier to learn and associate with the target class. In this work, we use the equivariance and invariance properties (Sec. 3.2) to increase the variance of t without adversely affecting prediction accuracy.

Most contrastive SSL methods (eg: [1, 5, 7]) incorporate some form of invariance conditioning in their training, which is the underlying reason behind the failure of backdoor attacks in SSL. However, certain backdoor attacks poison in the frequency space instead of the spatial space, thereby making the trigger invariant to spatial transformation. In this work, we investigate [11] and [4] (Sec. 8.2) as two frequency-based backdoor attacks. Such poison attacks can be defended simply by adding a frequency space augmentation in g , and to that end, we introduce *gaussian blur* to the set of augmentations. Gaussian blur is an invertible operation (if the parameters are known), and can be used in segmentation tasks without additional effort. Refer Sec. 4.2 for an analytical understanding of the relationship between blur and variance in frequency-based attacks. It is important to note that preliminary results already indicate Gaussian Noise can add robustness to the training. However, blur improves the performance of the model by forcing it to rely on overall semantic structure as compared to the lower-level features (fine-grain details) to make predictions, while also reducing the attack strength in a predictable manner.

All augmentations to be used, have a random probability of being applied to the image. Additionally, we also sample a random strength each time an image is blurred, in an attempt to maximize variance.

Augmentations for invariance. We use spatial transformations such as resized crop, horizontal flip, color jitter and grayscale in our experiments. These transformations defend against patch-based attacks ([19]), which are not spatial transformation invariant. As discussed, we add gaussian blur to g to defend against frequency-based attacks. We integrate the transformations in SSL's training process. Let \mathbf{x} be an input image. We randomly sample two compositions of transforms from list g_1 and g_2 ($g_1, g_2 \sim g$), and apply them on the input image \mathbf{x} .

$$\mathbf{x}_1 : g_1(\mathbf{x}) \quad \mathbf{x}_2 : g_2(\mathbf{x}) \quad (3)$$

The model (F_θ) is trained by minimizing a contrastive loss function \mathcal{L}_{con} between \mathbf{x}_1 and \mathbf{x}_2 .

Augmentations for equivariance. In addition to previously mentioned transformations, rotation and a few other invertible augmentations may be added to further strengthen defense in Segmentation/Detection tasks. Let \mathbf{x} be an input image. We consider all transforms from list g_i and apply them on the input image \mathbf{x} . The model (F_θ) is trained by minimizing an objective \mathcal{L}_{equi} on top of downstream task loss \mathcal{L}_{task} :

$$\begin{aligned} \mathcal{L}_{equi} : & \sum_{g_i \in g} d(F_\theta \circ g_i(\mathbf{x}), g_i \circ F_\theta(\mathbf{x})) \\ \text{or} \quad & \sum_{g_i \in g} d(g_i^{-1} \circ F_\theta \circ g_i(\mathbf{x}), F_\theta(\mathbf{x})) \end{aligned} \quad (4)$$

$$Loss(\mathcal{L}) : c_{equi} \cdot \mathcal{L}_{equi} + c_{task} \cdot \mathcal{L}_{task} + c_{reg} \cdot \mathcal{L}_{reg} \quad (5)$$

where \mathcal{L}_{reg} and c_{reg} represent regularization loss and coefficient/weight respectively, and d is any distance metric such as L_1/L_2 distances, negative cosine similarity, SSIM, etc.

4.2. Blur and frequency-based attacks

Consider a clean image x and its poisoned variant y . Let their blurred forms be represented as x_b and y_b . Considering our threat model (Sec. 4), an attacker can poison a fraction of the dataset. A potent backdoor attack would try to minimize the variance of trigger pattern while maintaining evasiveness. Generalizing dependence on x , let the trigger pattern in the frequency domain be represented as $t(x)$. For

FIBA and CTRL, $t(x)$ is defined as:

$$\begin{aligned} \text{CTRL} : t_{i,j}(x) &: \begin{cases} c & i = j \text{ and } i \in \{\frac{s}{2}, s\} \\ 0 & \text{otherwise} \end{cases} \\ \text{FIBA} : t_{i,j}(x) &: \begin{cases} \text{Mag}(x^f) & (i, j) \in \text{low freq. patch} \\ 0 & \text{otherwise} \end{cases} \end{aligned} \quad (6)$$

where $\text{Mag}(x)$ finds the magnitude of the complex number x . Poisoned image $y(x)$ is obtained as $\text{IFFT}(x^f + t(x))$. Blurred image x_b is obtained using a blur kernel k as $k * x$. Now y_b :

$$\begin{aligned} y_b &= k * y \\ &= k * \text{IFFT}(x^f + t(x)) \\ &= \text{IFFT}(k^f \cdot x^f + k^f \cdot t(x)) \\ &= \text{IFFT}(k^f \cdot x^f) + \text{IFFT}(k^f \cdot t(x)) \\ &= x_b + \underbrace{k * \text{IFFT}(t(x))}_{\text{trigger}} \end{aligned} \quad (7)$$

where, k^f represents $\text{FFT}(k)$. As discussed in Sec. 8.1, FIBA already has a poor ASR in SSL due to the variance present in $t(x)$. In CTRL $t(x)$ is not entirely independent of x . The authors *clamp* y to lie between $[0, 1]$, which is a non-linear operation. Therefore, the residual $r(x) = y - x$ (Fig. 1) varies with the image x . When $r(x)$ is blurred to get $r_b(x)$, its dependence (indicated by variance) on x is amplified. Even without clamp, randomly sampling blur strength adds enough variance in the residual $r_b(x)$ to impede its association with the target class instead of x_b .

4.3. Defense at inference using luma channel

Frequency domain attacks introduce a trigger pattern that covers the whole target image, and thus it is in the attacker's interest to keep the trigger as inauspicious as possible. Since human vision is most perceptive to luminance, this could be achieved by only poisoning the chromatic channels while making minimal modifications to the luma channel. Thus we assume that the Y' (luma) channel of a poisoned image will be relatively clean.

Let \mathbf{x}_{RGB} denote the original image, and $\mathbf{x}_{Y'}$ represent the image created by replicating the Y' channel (Eq. 2) obtained from \mathbf{x}_{RGB} to form a three-channel image. Our proposed defense strategy during inference involves utilizing $\mathbf{x}_{Y'}$ instead of \mathbf{x}_{RGB} for downstream tasks. In the case of poisoned samples, while $\mathbf{x}_{\text{RGB}}^{\text{pois}}$ would be positioned within the cluster corresponding to the target class irrespective of its actual class, $\mathbf{x}_{Y'}^{\text{pois}}$ would still reside within its actual class cluster (Fig. 2, 3). This resilience stems from the assumed minimal interference with the luma channel during the poisoning process. Consequently, this inference scheme effectively mitigates chroma-based poisoning attacks (Table 2).

Because the Y' channel retains all semantic information of an image, the embeddings generated by the poisoned model on $\mathbf{x}_{Y'}$ would maintain a cluster structure similar to the embeddings generated on \mathbf{x}_{RGB} (Fig. 2, 3). Thus the downstream classification task would not suffer from any noticeable loss in accuracy when performing inference on $\mathbf{x}_{Y'}$.

5. Experimental details

5.1. Datasets

We use the CIFAR 10 and CIFAR 100 datasets for all our experiments. We use the setup described in [19] to sample 100 classes from the Imagenet dataset. The CIFAR 10 and CIFAR 100 datasets are split into training (50,000 images) and testing (10,000 images) sets. CIFAR 10 contains 10 classes with 6,000 images per class, while CIFAR 100 contains 100 classes with 600 images per class. Following [11], we poison 1% of the training set in CIFAR 10 for all attacks. Since 1% of CIFAR 100 constitutes an entire class, we poison 0.4% of CIFAR 100. To maintain consistency, all results shown in the paper are based on experiments carried out by setting the target class as "1".

5.2. Encoder training

We use the training split of our dataset to train self-supervised encoders (SimCLR and BYOL) in a contrastive fashion. We use hyperparameters set by [11] for the encoder training process. Table 1 lists the key hyperparameters used in Encoder training.

Hyperparameter	SimCLR	BYOL
Optimizer	SGD	SGD
Learning Rate	0.06	0.06
Momentum	0.9	0.9
Weight Decay	5×10^{-4}	5×10^{-4}
Epochs	800	800
Batch Size	512	512
Temperature	0.5	–
Moving Average	–	0.996

Table 1. Hyperparameters for SSL Methods (SimCLR, BYOL)

5.3. Classification metrics

Following [24], we use the metrics ACC (clean accuracy) to measure a backdoored classifier's performance on classifying clean samples, and ASR (Attack success rate) to evaluate the backdoor attack efficacy of the overall setup. ASR is defined as the percentage of poisoned samples that are classified as the target class.

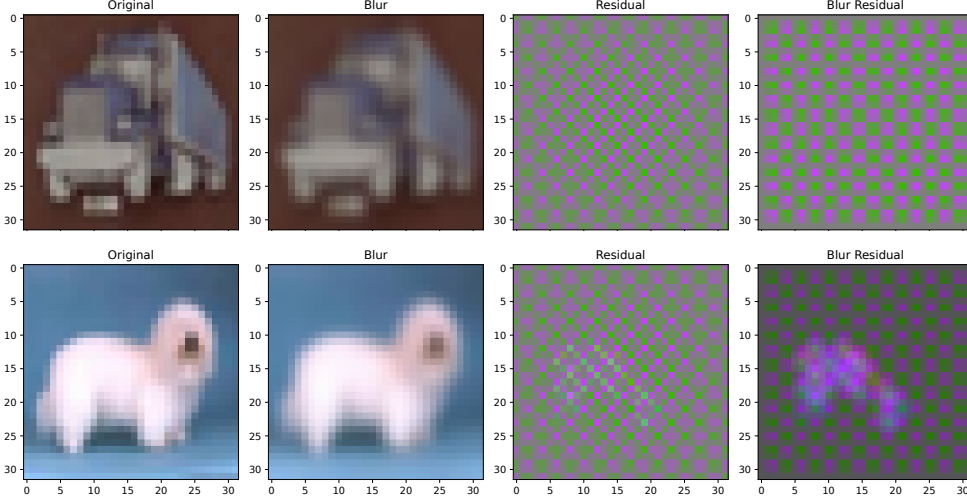


Figure 1. Example of CTRL attack on two different images. The residual r remains mostly identical for different images, thereby providing a path of least variance. Blurring the poisoned image y results in a residual r_b which varies between images.

5.4. Classifier training

Following [11], we use K-Nearest Neighbours on the embeddings generated by SSL encoder for our classification task. We calculate the ACC using the entire testing-set (10,000 samples). To find the ASR, we consider the testing-set poisoned as a whole using the backdoor attack under consideration (CTRL/FIBA/HTBA).

6. Results and discussions

We present our results in Table 2. SSL encoder(s) trained with RGB images generate meaningful embeddings in other color spaces that maintain semantic information. Results indicate that classification in luma-space (Y') reduces ASR to a point where it cannot be distinguished from random-chance (equiprobable for all classes), without a noticeable drop in prediction accuracy on clean samples. Note that inference on the full $Y'UV$ images leads to an increase in ASR because the poison trigger becomes more pronounced in U and V channels. We also observe that contrastive training with blur provides a two-fold benefit: ACC is notably increased while ASR is reduced by 60 - 85% depending on the dataset and method. For best results, we recommend using both strategies in conjunction.

7. Further experiments

7.1. Visualizing poison distribution in learned representation spaces

Here, we demonstrate through scatter plots how the poisoned embeddings are distributed with respect to the complete data landscape for CIFAR 10. For the CIFAR 10 test

dataset (10,000 images, 1000 images per class), we randomly sample 1000 indices and poison these images. We use a combination of PCA ($n_components = 50$) followed by a t-SNE dimensionality reduction to represent the data in two dimensions. We observe that the poison embeddings greatly overlap with the target class in the ‘RGB’ case(s) (Fig. 2, 3), making the backdoor attack quite effective. However, in case of Luma, the poison embeddings appear distributed across the data landscape in a disjointed fashion. This indicates failure of backdoor attack, and demonstrates a visual reasoning behind the success of our defense.

7.2. Performance of clean models

We present in Table 3, results on models trained with clean data. For the sake of consistency, we use same hyperparameters for models with and without defense. We observe that blur further enhances KNN accuracy by a noticeable amount.

7.3. Inference on other color-spaces

We try inference time defense on various different color-spaces which have a channel that is analogous to the luma channel (Y') present in $Y'CbCr$, $Y'UV$ etc. For this we select the value channel V from HSV , and the lightness channels L from HSL , LUV and LAB color-spaces. Note that the L channels from LUV and LAB are the same. We follow the scheme given in Sec. 4.3 to construct new three channel images after performing the respective color-space transformations. The results of backdoor attack on these transformed images is summarised in Table 4.

The transforms maintain the cluster structure and thus have similar KNN accuracy as the original RGB image.

Method	Dataset	RGB		Y'UV		Y'		RGB (Blur)	
		ACC	ASR	ACC	ASR	ACC	ASR	ACC	ASR
SimCLR	CIFAR 10	84.96	83.62	82.02	98.29	83.94	10.36	89.38	35.54
	CIFAR 100	49.76	95.5	45.44	97.78	47.19	3.22	56.24	38.98
BYOL	CIFAR 10	86.36	91.31	83.76	99.09	85.11	11.13	90.45	19.22
	CIFAR 100	51.71	92.93	48.58	98.94	48.97	2.98	59.36	14.96
SimSiam	CIFAR 10	85.34	59.36	NA	NA	NA	NA	89.32	15.51
	CIFAR 100	55.08	86.76	NA	NA	NA	NA	60.34	40.63

Table 2. Comparison of defense against CTRL attack

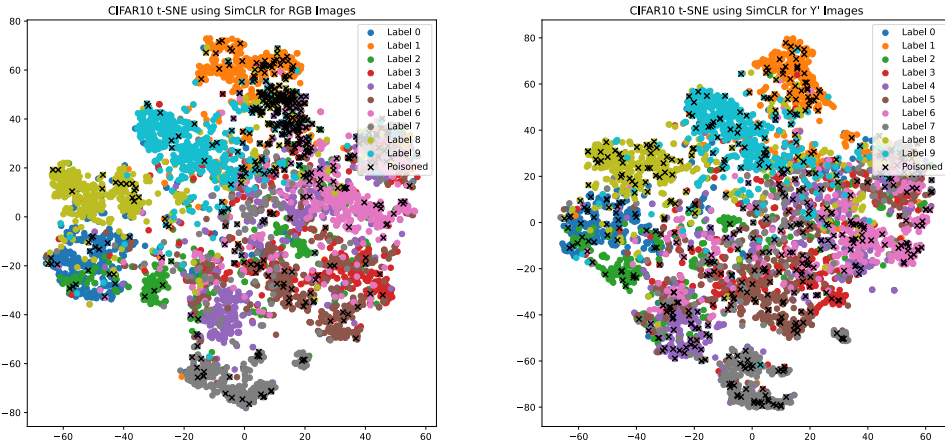


Figure 2. t-SNE Clustering on SimCLR using (left) RGB and (right) Y' images display attack and defense.

Method	Dataset	ACC (%)	
		Without Blur	With Blur
SimCLR	CIFAR 10	84.73	89.34
	CIFAR 100	48.36	55.94
BYOL	CIFAR 10	86.19	90.36
	CIFAR 100	52.41	59.93
SimSiam	CIFAR 10	85.71	89.50
	CIFAR 100	53.64	59.25

Table 3. Performance of models on clean dataset

However unlike inference on Y' , we do not observe any appreciable decrease in ASR with inference on V or the L channels. This is due to the fact that Y' encodes a color image taking human perception into account, whereas transformations like HSV and HSL seek to turn a color model into three components: the lightness, the colorfulness, and the hue. Thus the V and L channels still carry the poison

trigger pattern unlike Y' as shown in Fig. 4.

8. Exploring other attack strategies against SSL

8.1. FIBA: A frequency-injection based backdoor attack

FIBA was introduced by [4], as a frequency injection based backdoor attack against medical image segmentation.

Let K_{x_i, x^t} be the poisoning filter in frequency domain, with its spatial domain function representation k_{x_i, x^t} . According to [4], K_{x_i, x^t} is defined as

$$K_{x_i, x^t} = \begin{cases} f(m, n) & (m, n) \in \text{low freq. patch} \\ 1 & \text{otherwise} \end{cases} \quad (8)$$

where,

$$f(m, n) = \frac{(1 - \alpha)\mathcal{F}_{x_i}^A(m, n) + \alpha\mathcal{F}_{x^t}^A(m, n)}{\mathcal{F}_{x_i}^A(m, n)} \quad (9)$$

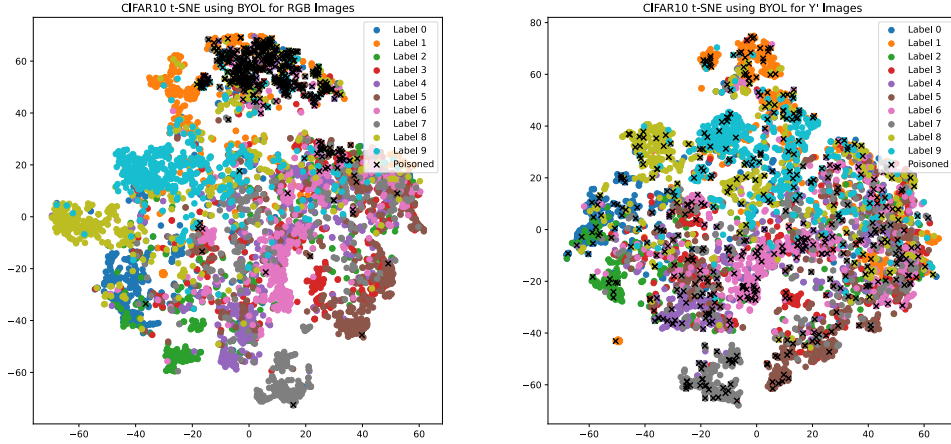


Figure 3. t-SNE Clustering on BYOL using (left) RGB images display the attack, (right) Y' images display the defense.

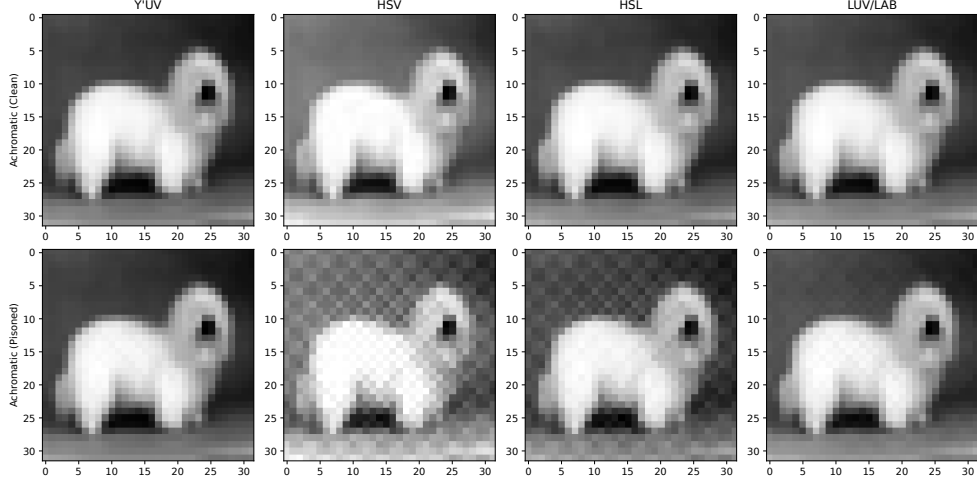


Figure 4. The achromatic channels of various color-spaces for clean and poisoned images.

Thus the poisoned image x_i^p is a convolution of k_{x_i, x^t} and the input image (x_i). Since the filter k is dependent on the image x_i and consequently will change for each image, the poisoning will have a high variance. This is illustrated in Fig. 5 where the residuals change for different x_i . Hence the poisoned images will fail to form a cluster that overlaps with the target class under SSL training, leading to poor ASR (Table 5).

8.2. Hidden trigger backdoor attacks (HTBA): a patch-based attack strategy

[19] demonstrate patch-based attacks against SSL. Their attack strategy, (HTBA) introduces small trigger patches into a small subset of target class images. They theorize that the model prefers to associate the easier-to-learn triggers with

the target class rather than through semantic understanding of the image. They also note that their attack would be ineffective if the trigger were lost during augmentations, which is a mandatory step for SSL. We present results using their poisoning strategy below.

9. Conclusion

This work conducts a systematic study on the adversarial robustness of SSL against backdoor attacks. We reveal the fundamental understanding behind the working of a backdoor attack through the concept of variance (Sec. 4.1) and devise a defense strategy based on it. By proving our defense's effectiveness in SSL, we lay the foundation for robustness against backdoor attacks in other paradigms

Method	Dataset	RGB		V (HSV)		L (HSL)		L (LUV/LAB)	
		ACC	ASR	ACC	ASR	ACC	ASR	ACC	ASR
SimCLR	CIFAR 10	84.96	83.62	84.31	90.99	83.88	95.30	84.09	59.24
	CIFAR 100	49.76	95.5	47.03	93.09	46.96	96.63	47.72	69.09
BYOL	CIFAR 10	86.36	91.31	85.04	83.0	84.90	92.95	85.29	62.8
	CIFAR 100	51.71	92.93	48.44	87.66	48.29	92.14	49.32	58.72

Table 4. Comparison of defense against CTRL attack using other color-spaces

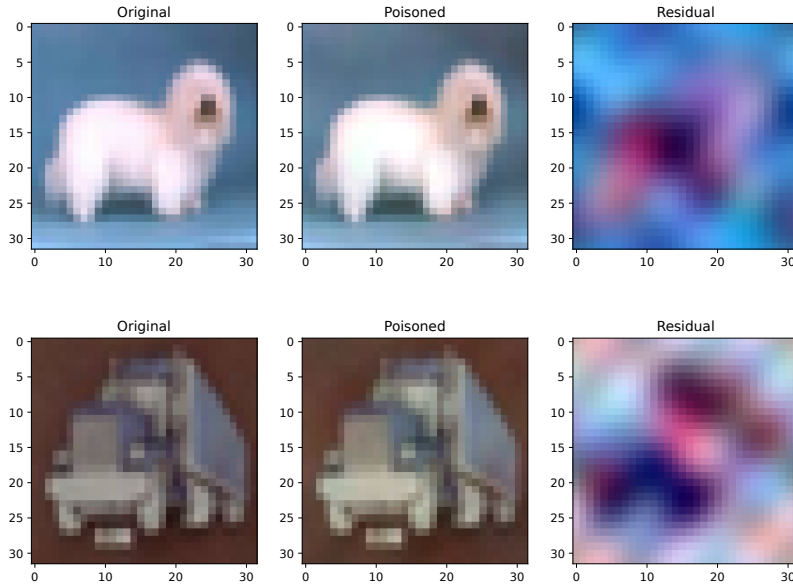


Figure 5. Example of FIBA poisoning on two different images. The residuals, i.e. the difference between original and poisoned image vary between images. Scaled version of residuals have been plotted for visualization purposes.

Method	Dataset	Without Blur		With Blur	
		ACC	ASR	ACC	ASR
SimCLR	CIFAR 10	84.96	9.948	89.52	10.06
	CIFAR 100	48.51	0.906	56.32	1.046
BYOL	CIFAR 10	85.98	10.14	90.32	10.21
	CIFAR 100	52.23	0.83	59.77	0.948

Table 5. Comparision of defense on FIBA

Method	Dataset	Without Blur		With Blur	
		ACC	ASR	ACC	ASR
SimCLR	CIFAR 10	84.36	17.3	89.08	17.39
	CIFAR 100	49.03	16.61	56.35	12.76
BYOL	CIFAR 10	85.69	17.59	90.39	16.41
	CIFAR 100	51.71	22.63	59.85	18.67

Table 6. Comparision of defense on HTBA

of learning, such as Supervised Learning, and we hope to achieve this in a subsequent paper. We hope our findings will shed light on generalized defense strategies against backdoor attacks and encourage the community to consider backdoor vulnerabilities while training.

10. Limitations

While the literature on backdoor attacks against Supervised-Learning is abundant, very little research exists on backdoor attacks targetting SSL, owing to the adversarial robustness of SSL and the absence of labels for training. This work tests our defense against CTRL, FIBA, and HTBA. Due to

time constraints, we could only evaluate our work in CIFAR 10 and CIFAR 100. We plan to conduct our experiments on other datasets (e.g. Imagenet100 which was introduced in [19]) and SOTA foundation models (e.g. MoCo v3, SimSiam). For our experiments, we follow all hyperparameters available from [11] and appropriately assign values to the remaining, which is not necessarily optimal. The future scope of this research includes extending the attack and the defense to multi-modal SSL regimes, e.g., CLIP. Additionally, theoretical understanding behind the working of backdoor attacks in terms of invariance and equivariance, opens room for researchers to find the optimal trigger pattern which is resistant to defenses.

References

- [1] Ting Chen, Simon Kornblith, Mohammad Norouzi, and Geoffrey Hinton. A simple framework for contrastive learning of visual representations. In *Proceedings of the 37th International Conference on Machine Learning*, pages 1597–1607. PMLR, 2020. [1](#), [3](#)
- [2] Xinlei Chen and Kaiming He. Exploring simple siamese representation learning, 2020. [1](#)
- [3] Xinyun Chen, Chang Liu, Bo Li, Kimberly Lu, and Dawn Song. Targeted backdoor attacks on deep learning systems using data poisoning. *arXiv preprint arXiv:1712.05526*, 2017. [1](#)
- [4] Yu Feng, Benteng Ma, Jing Zhang, Shanshan Zhao, Yong Xia, and Dacheng Tao. Fibia: Frequency-injection based backdoor attack in medical image analysis. In *Proceedings of the IEEE/CVF Conference on Computer Vision and Pattern Recognition*, pages 20876–20885, 2022. [2](#), [3](#), [6](#)
- [5] Jean-Bastien Grill, Florian Strub, Florent Altché, Corentin Tallec, Pierre H. Richemond, Elena Buchatskaya, Carl Doersch, Bernardo Avila Pires, Zhaohan Daniel Guo, Mohammad Gheshlaghi Azar, Bilal Piot, Koray Kavukcuoglu, Rémi Munos, and Michal Valko. Bootstrap your own latent: A new approach to self-supervised learning, 2020. [1](#), [3](#)
- [6] Tianyu Gu, Brendan Dolan-Gavitt, and Siddharth Garg. Badnets: Identifying vulnerabilities in the machine learning model supply chain, 2019. [1](#)
- [7] Kaiming He, Haoqi Fan, Yuxin Wu, Saining Xie, and Ross Girshick. Momentum contrast for unsupervised visual representation learning. *arXiv preprint arXiv:1911.05722*, 2019. [1](#), [3](#)
- [8] S Hemalatha, U Dinesh Acharya, and A Renuka. Comparison of secure and high capacity color image steganography techniques in rgb and ycbcr domains. *arXiv preprint arXiv:1307.3026*, 2013. [2](#)
- [9] Jinyuan Jia, Yupei Liu, and Neil Zhenqiang Gong. BadEncoder: Backdoor attacks to pre-trained encoders in self-supervised learning. In *IEEE Symposium on Security and Privacy*, 2022. [2](#)
- [10] Huang Kunzhe, Li Yiming, Wu Baoyuan, Qin Zhan, and Ren Kui. Backdoor defense via decoupling the training process. In *ICLR*, 2022. [2](#)
- [11] Changjiang Li, Ren Pang, Zhaohan Xi, Tianyu Du, Shouling Ji, Yuan Yao, and Ting Wang. An embarrassingly simple backdoor attack on self-supervised learning. In *Proceedings of the IEEE/CVF International Conference on Computer Vision (ICCV)*, pages 4367–4378, 2023. [1](#), [2](#), [3](#), [4](#), [5](#), [9](#)
- [12] Shaofeng Li, Minhui Xue, Benjamin Zi Hao Zhao, Haojin Zhu, and Xinpeng Zhang. Invisible backdoor attacks on deep neural networks via steganography and regularization. *IEEE Transactions on Dependable and Secure Computing*, 18(5): 2088–2105, 2020. [1](#)
- [13] Yige Li, Xixiang Lyu, Nodens Koren, Lingjuan Lyu, Bo Li, and Xingjun Ma. Neural attention distillation: Erasing backdoor triggers from deep neural networks. In *ICLR*, 2021. [2](#), [3](#)
- [14] Hongbin Liu, Jinyuan Jia, and Neil Zhenqiang Gong. {PoisonedEncoder}: Poisoning the unlabeled pre-training data in contrastive learning. In *31st USENIX Security Symposium (USENIX Security 22)*, pages 3629–3645, 2022. [2](#)
- [15] Chengzhi Mao, Lingyu Zhang, Abhishek Vaibhav Joshi, Junfeng Yang, Hao Wang, and Carl Vondrick. Robust perception through equivariance. In *Proceedings of the 40th International Conference on Machine Learning*, pages 23852–23870. PMLR, 2023. [2](#)
- [16] Lu Pang, Tao Sun, Haibin Ling, and Chao Chen. Backdoor cleansing with unlabeled data. In *CVPR*, 2023. [2](#)
- [17] Joseph Rance, Yiren Zhao, Ilia Shumailov, and Robert Mullins. Augmentation backdoors, 2022. [2](#)
- [18] Aniruddha Saha, Akshayvarun Subramanya, and Hamed Pirsiavash. Hidden trigger backdoor attacks. In *Proceedings of the AAAI conference on artificial intelligence*, pages 11957–11965, 2020. [2](#)
- [19] Aniruddha Saha, Ajinkya Tejankar, Soroush Abbasi Koohpayegani, and Hamed Pirsiavash. Backdoor attacks on self-supervised learning. In *Proceedings of the IEEE/CVF Conference on Computer Vision and Pattern Recognition*, pages 13337–13346, 2022. [2](#), [3](#), [4](#), [7](#), [9](#)
- [20] Daniela Stanescu, Mircea Stratulat, Voicu Groza, Joana Ghergulescu, and Daniel Borca. Steganography in yuv color space. In *2007 International Workshop on Robotic and Sensors Environments*, pages 1–4, 2007. [2](#)
- [21] Mingjie Sun and Zico Kolter. Single image backdoor inversion via robust smoothed classifiers. *Proceedings of the IEEE/CVF Conference on Computer Vision and Pattern Recognition (CVPR)*, 2023. [2](#)
- [22] Ajinkya Tejankar, Maziar Sanjabi, Qifan Wang, Sinong Wang, Hamed Firooz, Hamed Pirsiavash, and Liang Tan. Defending against patch-based backdoor attacks on self-supervised learning. In *Proceedings of the IEEE/CVF Conference on Computer Vision and Pattern Recognition*, pages 12239–12249, 2023. [2](#)
- [23] G.K. Wallace. The jpeg still picture compression standard. *IEEE Transactions on Consumer Electronics*, 38(1):xviii–xxxiv, 1992. [2](#)
- [24] Bolun Wang, Yuanshun Yao, Shawn Shan, Huiying Li, Bimal Viswanath, Haitao Zheng, and Ben Y. Zhao. Neural cleanse: Identifying and mitigating backdoor attacks in neural networks. In *2019 IEEE Symposium on Security and Privacy (SP)*, pages 707–723, 2019. [2](#), [4](#)

- [25] Kota Yoshida and Takeshi Fujino. Countermeasure against backdoor attack on neural networks utilizing knowledge distillation. *Journal of Signal Processing*, 24(4):141–144, 2020.
[2](#), [3](#)
- [26] Jure Zbontar, Li Jing, Ishan Misra, Yann LeCun, and Stéphane Deny. Barlow twins: Self-supervised learning via redundancy reduction. In *International Conference on Machine Learning*, pages 12310–12320. PMLR, 2021. [1](#)